Functional Texture Design and Texturing Processes

Nobuyuki Moronuki [*1]

[*1]Tokyo Metropolitan University, 6-6 Asahigaoka, Hino-shi, Tokyo 191-0065 Japan
E-mail: moronuki@tmu.ac.jp

Abstract. Various functions can be obtained by applying regular patterns or texture on a surface. Depending on the functions, required dimension of the texture, e.g. pitch, varies in wide range from nanometers for optical function to millimeters for friction. In addition, high aspect ratio of the cross sectional profile or hierarchical structure of micro-/nano-structure is required for example to control the wettability. This paper reviews various processes for functionalities including their applications.

Keywords: texture, functionality, processes, top-down, bottom-up

1. INTRODUCTION

Regular micro/nanostructures and textures provide such functions as optical and friction properties, but neither textural design nor the texturing process has been well established. Functional texture is often inspired by natural designs, typically a microstructure on a lotus leaf or the nanostructure of a gecko's foot. Biomimetic has become a key word in state-of-the-art technologies relevant to surface functionality.

Processes for texturing are also important because functional texture requires a wide range of structural dimensions from nanometers to micrometers. Top-down processes such as cutting or energy beam processing are popular and are based on the copying rule, thus, the relative motion between tool and workpiece is copied to the workpiece. On the other hand, bottom-up processes include the self-assembly of particles and the anodic oxidation of aluminum. The principle behind these differs completely from that of top-down processes, thus, the results have a certain randomness in nature.

In addition, material deposition can change surface functionalities. These considerations make a comprehensive understanding necessary from texturing and material basics to applications in various fields.
This paper surveys these trends in design and processing, introducing key examples in each field.

2. ATTAINABLE FUNCTIONS AND DESIGN

2.1. Attainable Functions

Nature is often referred in the discussion of surface function. With the progress of measurement instruments like scanning election microscope, functional structure or texture had been revealed.

Table 1 summarizes the attainable functions with texture. The applied fields are wide spread. The object that contact with the texture is not only limited to liquid and solid, but living tissue is also included. Regenerating medicine is expected to cultivate a big market in future. Electromagnetic wave interaction with the texture may also have potential market in future. Some of these application will be introduced later.

Fig. 1 shows the observation results of the gecko's foot [1]. In millimeter scale it has lamella structure, and in nanometer scale it has branched fibers at the tips to increase the number of contact points [2]. The principle of the adhesion of the foot is van der Waals force. The individual attraction force is of course weak, however, increasing the number of contact points it can walk on a wall for example holding its own weight.

Table 1 Various functions and applications related to textured surfaces

Object	Functions	Applications
Liquid	Wettability	Self-cleaning, ice/snow anti-stick
	Drag reduction	Pipeline, efficient ship
	Filter	Gas/liquid separation
Solid	Friction	Anti-stiction of HD head, safe floor of pool/bath
	Tactile	Handle surface
	Surface area	Catalyst, gas sensor
	Biocompatibility	Implant, artificial organ
Electro-Magnetic wave	Transmission	Antireflective, solar panel
	Reflection	Road sign, mouse pad
	Diffraction/ interference	Spectroscope, hologram

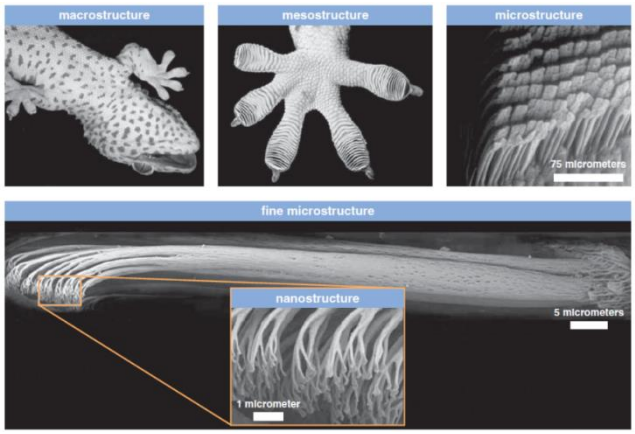

Fig. 1 Gecko's foot has branched nanostructures at the tip to gather weak attraction force of each contact with wall to hold its own weight [1].

Fig. 2 shows the photos of droplet on a leaf [3] and moth eyes [4]. It is well known that lotus leaf repels water droplet or hydrophobic and keep the surface clean. It is reasonable, considering species preservation, to maximize the efficiency of photosynthesis. It was already found that the lotus leaf has complex structure of micrometer level and nanometer level.

On the other hand, moth eye has nanometer scale texture on the surface, which decreases the reflection as shown in **Fig.3**. It is well known that the eye function of moth had atrophied, but they have such function to maximize the incoming light intensity while minimizing the reflecting light. It is also found from the photo that there are many hairs in submillimeter size. These hair seems to have water repelling function to keep the eye sight clear.

2.2. Design of Textures

Various functions are observed in nature described above and all of these can be utilized or mimicked for industrial design. **Fig. 4** shows an example of bioinspired or biomimetic design [5]. Depending of the structural size, from nanometer to millimeter, wide spectrum of functions are realized. Fine and dense structure works as barrier for specific material transportation. The wettability control, self-cleaning, and optical functions are already described. Surface structure also affects the heat dissipation effect. All of these functions can be applied in specific devices or products [6].

One of the problems is that design methodology has not been established. From the observation of nature, the structure or dimension can be identified. However, the source material is absolutely different. Many natural object is made from proteins, while industrial product are mostly made of metals. It should be noted that natural material like spider's thread has better mechanical property than synthetic fibers such as Nylon® [2]. In addition to the material difference, a design that compromise plural functions is very difficult.

Wetting and sliding of liquid on a surface is sometime difficult to understand because the mechanism is complicated. Wetting of a liquid on a surface is often compared using the contact angle (CA). Ideally, it can be controlled with surface energy of the surface. The effect of texture have been made clear [7], [8] referring Cassie-Baxter theory [9] and its extension [10]. In addition to the surface texture, the effect of material was also made clear [11].

On the other hand, sliding or movement mechanism of a droplet on a surface becomes complicated because the work done by the movement contact line should be taken into account in addition to static equilibrium conditions of interfacial forces. Pinning effect, discontinuity of cross-section or the chemical composition pins the movement of a droplet is pinned just like to pin a paper on a board, makes the mechanism complicated further.
The mobility of a droplet can be measured by a sliding angle or the hysteresis calculated by the difference between advancing contact angle and receding angle. The effect of chemical modification of the texture on the hysteresis was already discussed [12]. The formulation of sliding angle was also discussed [13].

Fig. 5 shows an example for anti-fouling surface inspired by the nepenthes leaves. Nepenthes is one of the insectivorous plants of which surface is covered with a liquid. An insect cannot hold on it and slide down and then predated. To mimic this design, porous structure was prepared and liquid was infused [14]. After the infusion, not only the solid but liquid slide down easily.

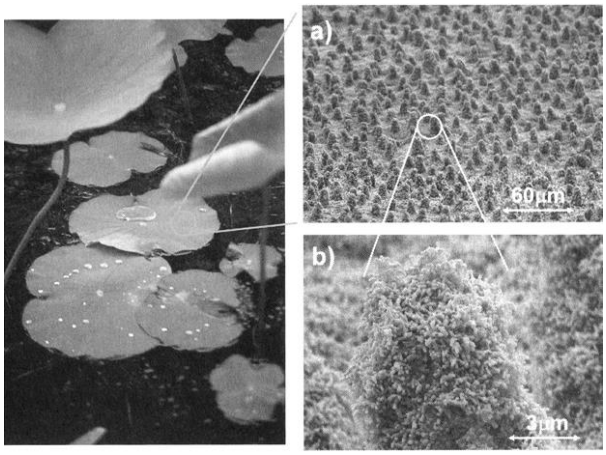

Fig. 2 Droplet on a leaf showing its hydrophobicity (left). It is attained by the hierarchical structure in micro-level (a) and nano-level (b) on the surface [3].

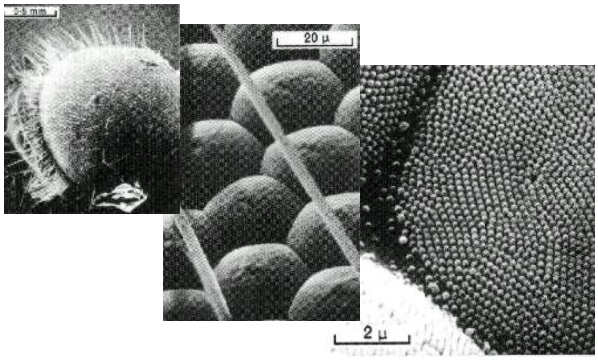

Fig. 3 Moth eye showing antireflectivity due to nanostructures on the surface [modified from ref.4].

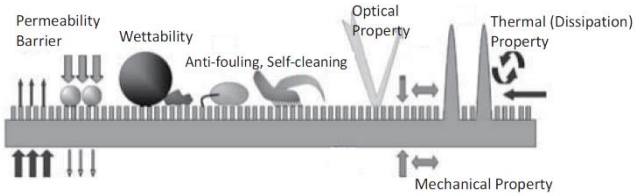

Fig. 4 Schematics of various surface functions based on bioinspired design [5].

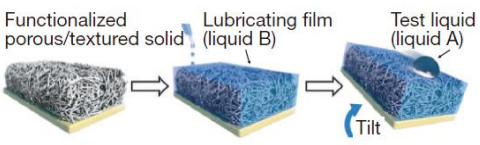

Fig. 5 Slippery surface design inspired by the nepenthes leaves. Infused with a special liquid (B) on the surface can repels liquid (A) thus anti-fouling surface attained [14].

Fig. 6 shows the verification results referred from [14]. It shows the relationship between surface tension of the liquid and contact angle hysteresis which is defined in the inset of the figure. The hysteresis is directly related to sliding angle, thus, droplet easily slides down on a smaller hysteresis surface. With the decrease in surface tension, the hysteresis tends to increase. However, it is found that the hysteresis was kept small on the SLIPS. The term "SLIPS" is the abbreviation of slippery liquid infused porous surface(s). The "Ref. 9" corresponds to [15] in this paper. With the help of mobility of infused oil, the functionality can be recovered from physical damage. However, surface texture is important to elongate the functional life.

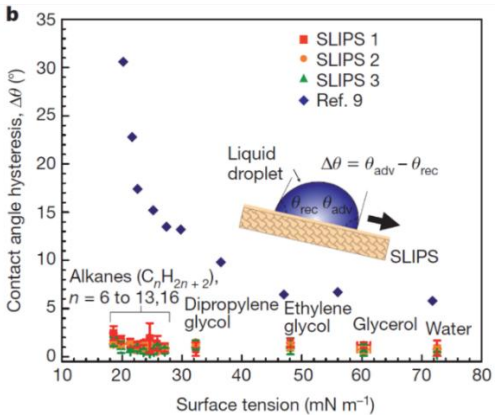

Fig. 6 Verification of self-cleaning function with low surface tension liquid. Small hysteresis indicates the easiness of droplet mobility on a solid surface [14].

3. TEXTURING PROCESSES

Table 2 shows the variation of the processes for texturing. Processes are divided into two categories: Top down or bottom up. The principle of the top down processes is the copying rule. The accuracy of the machine or mask is copied to the products, while the principle of the bottom up process depends on the self-organizing principle. In top down category, deposition processes are included in addition to the traditional machining processes. In these processes, the material is not limited to metals but various kind of polymers or chemical or organic materials are involved.

Table 2 Various processes for texturing. Both of top down and bottom up processes are included to cover wide range of dimensions.

Category		Example
Top down processes	Removal	Cutting, grinding, blast
		Electron, ion, laser
	Deformation	Emboss, imprint
	Deposition (thick)	Electroforming, CVD, PVD
	Deposition (thin)	Langmuir-Blodgett film, self-assembled monolayer, grafted polymer
Bottom up processes	Artificial	Self-assembly of particles, anodic oxidation of aluminum
	Natural	DNA, protein

Fig. 7 shows a rough comparison between the processes for texturing. Each process is shown as a rectangle showing the horizontal resolution and range both in horizontal or lateral direction and vertical or depth direction. For example, cutting process roughly have several tens micrometer horizontal resolution and submicron vertical resolution over meter range. On the other hand, so-called silicon process is difficult to indicate its area because any combination of patterning process like lithography and processes (removal or deposition) are possible. Thus, only the horizontal or vertical lines are indicated in the figure.

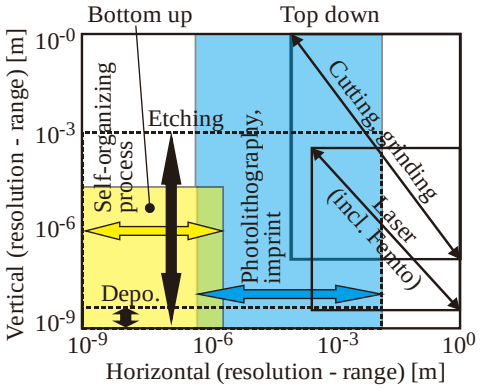

Fig. 7 Resolution and range of various processes along horizontal and vertical direction.

3.1. Top down Processes

3.1.1 Cutting

Traditional cutting processes can be used to texturing. First example is diamond micro-chiseling (DMC) [16], in which multi-axis and complex control is required as well as special tool. **Fig. 8** shows both of the schematics and machined example. Utilizing this process, optical reflective texture can be obtained. Replication of the texturing becomes important because the production rate is limited due to complicated machining process and slow cutting speed.

Second example is the application of fast tool servo mechanism [17][18]. Special setup is necessary to control the depth of cut dynamically to produce fine and regular patterns on the surface [19]. So far, improvement in both of frequency bandwidth and stroke of the tool motion was carried out. It has been also applied to hard-to-machine materials [20].

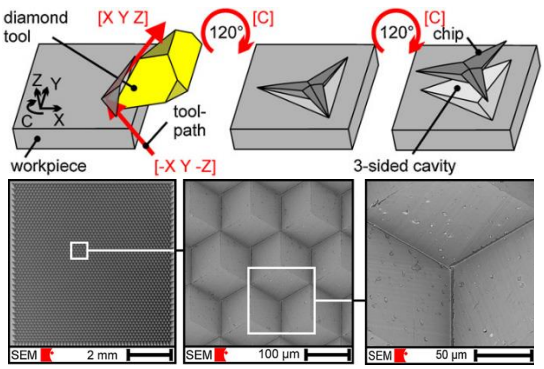

Fig. 8 Schematics of Diamond Micro-Chiseling (DMC) (upper) and SEM observation results (lower) [16].

Improvement in depth control up to nanometer level results in an optical element machining as shown in **Fig. 9** [17]. The bandwidth limits the throughput of the process because the depth of the tool should be controlled synchronizing with the rotation angle of the workiece. Typically, X kHz have been obtained. By using this setup, one kind hologram production can be possible with this process. Incorporating sensors, the reliability of the fast tool servo systems can be improved [21].

3.1.2 Grinding

It is not easy to apply grinding process to texturing because spatial frequency or pitch size of the regular profile is limited. However, this process can be applied to heat treatment [22]. The broad send of texturing includes modification of material properties as well as the modification of cross-sectional profile. Thus, material hardening with grinding process can be considered as one of the texturing processes.

From the standpoint of material hardening, rolling process should also be included [23].

3.1.3 Etching

Etching is one of the popular texturing processes. This process depends chemical reaction instead of hard tools, thus, there is no limitation of the workpiece material. For example, silicon carbide (SiC) has good mechanical properties such as high temperature strength. Balk machining like lapping is often applied to obtain flat surfaces. Fine and regular profile can be produced by applying conventional lithographic patterning with a mask and etching process. **Fig. 10** shows the texture on SiC substrate [24]. In this case, reactive ion etching (RIE) was adopted. This process combines the effect of ion bombardments and chemical etching by radicals. It has been made clear that texture on a bearing surface made by etching process can improve the bearing performance in water as shown in **Fig. 11**.

Anisotropic etching [25] is often applied to bulk micromachining of silicon substrate. Typical etchant is solution of potassium hydroxide (KOH) or tetramethylammonium hydroxide (TMAH) and the regular profile that consist of crystal plane {111} because this plane has the lowest surface energy among other planes. Pyramidal shape can be easily obtained and applied to improve solar cells performance [26]. Different etching processes can be combined to obtain special cross-sectional profile. For example, hiearchical structure is similar to that of lotus leaves [27].

Metal assisted chemical etching can produce specific profiles [28]. The principle of this etching is a catalytic reaction between noble metal deposited and silicon substrate and detailed process have been made clear [29], and high aspect ratio can be obtained with ease.

Fig. 12 shows an example of metal-assisted chemical etching. In this case, patterning was carried out with a shpere lithography. Self-assembled particles were used as a mask and a silver film with regular pores was deposited on the substrate. This film worked as a catalyst and selectively etched silicon substrate. Typical etchant is mixture of fluolic acid (HF) and hydrogen peroxide water (H_2O_2). Finaly, silicon pillars were obtained as shown in a SEM photo in (b).

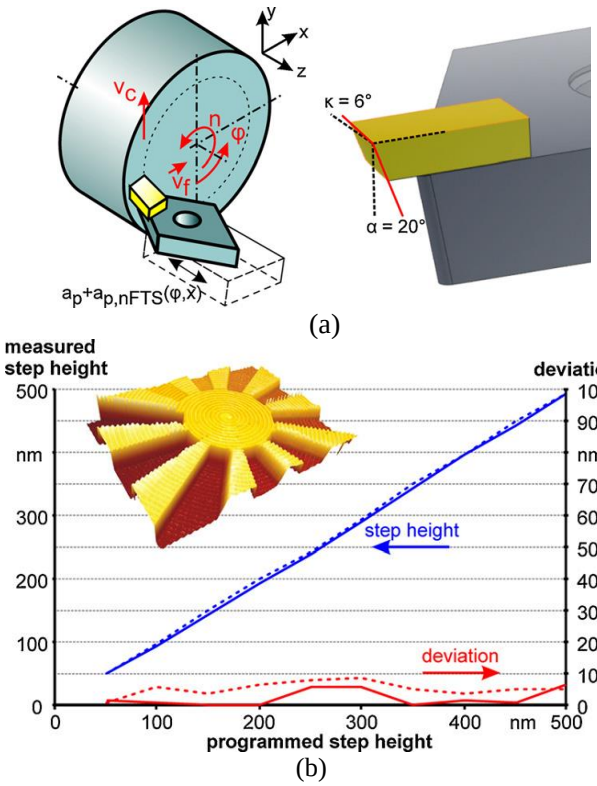

Fig. 9 Fast tool servo system applied for turning operation (a), and measurement result of step height synchronized with the workpiece rotation (b)[17].

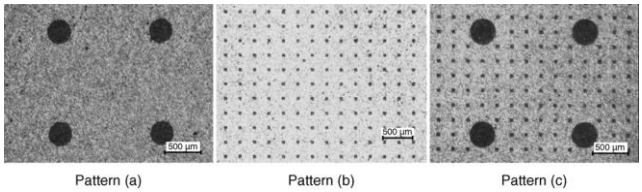

Fig. 10 Texture produced to decrease friction between the mating surfaces made of SiC [24]. Large dimples (a), small dimples (b) and the mixture (c). Depth is about 3-8 μm.

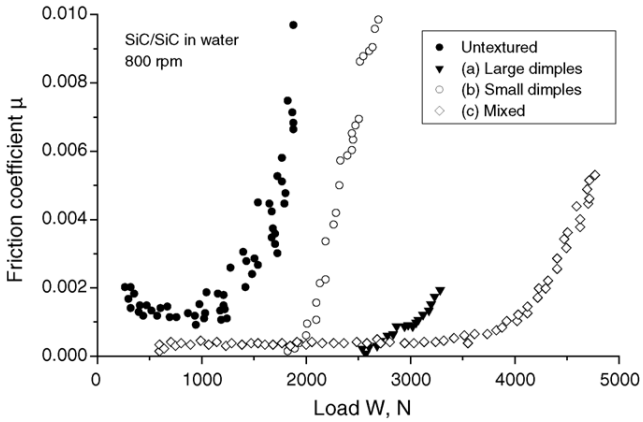

Fig. 11 Relationship between normal load and friction coefficient showing the effect of texturing. It can be found that texture improved the bearing performance [24].

In this process, sphere diameter was decreased with etching to decrease the pillar diameter while keeping the same pitch between them. By changing this diameter, the appearance of the texture changes from pillars to pores in bulk substrate. It is found from the SEM photo that pararrel pillars stand independently. However, with the increase in the aspect ratio of the pillar, the pillars get together like a bundle or bunched due to meniscus force between the pillars during the drying process. Based on the principle, there is no limtation in aspect ratio but it is limited in practice.

Textured surface often decrease reflectance and improves absorptivity of the surface. This property is preferable for the surface of photovoltaic devices. A review paper introduces many examples [29]. Of course, metal-assisted chemical etching is often applied for this aim [30].

Fig. 13 introduces a combination of metal-assisted chemical etching and another etching process for the improvement of photovoltaic devices [31]. Metal-assisted chemical etching was applied over limited area, and both of the bunched nanowires (NWs) and microwires (MWs) are obtained as shown in (a) left side. Then nanopillars were shortened with alkaline etching until short nano pillars covered the space between micro-pillars as shown in (a) right side. SEM photo (c) shows the actual structure as intended. It is considered that the light irradiated on this structure reflected between the micropillars sidewall and absorbed at the bottom of the spacing between them. This kind of co-integrated nano- and micro-wire (CNMW) solar cell shows the remarkably low reflectance, which suggest higher photovoltaic performance.

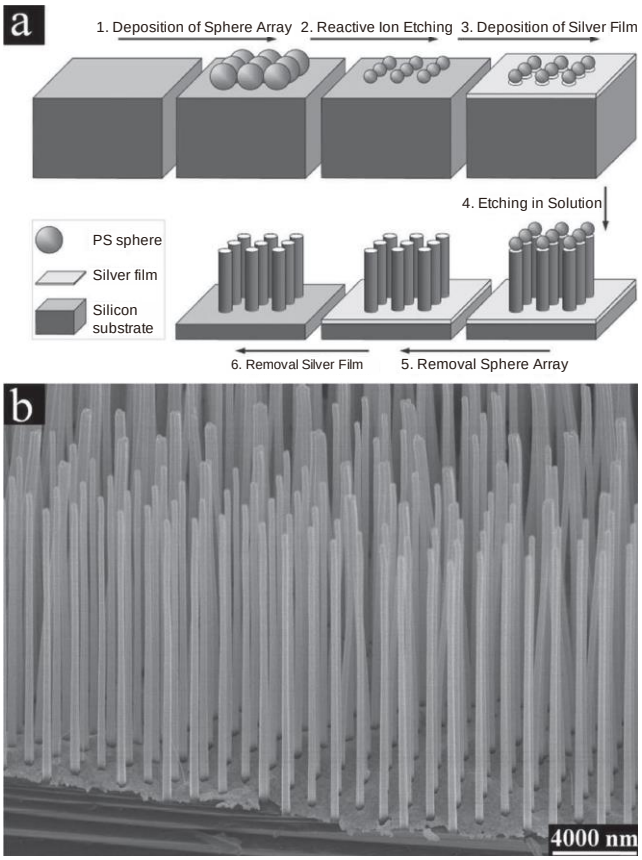

Fig. 12 Combination of nanosphere lithography and metal-assisted chemical etching. Polystyrene particles were assembled on a substrate and dry etched to decrease the diameter (a). Then, silver film was deposited and metal-assisted etched to obtain silicon pillars with high aspect ratio (b) [28] (partially modified).

In addition to applying texture on a surface, impregnation of special oil can change the spreading of liquid drastically. **Fig. 14** shows the observation results of the textured surface aiming for improvement of heat transfer coefficient [32]. Figure (a) shows vapor-deposited alumina-silica nanotexture, (b) shows re-entrant superomniphobic texture, (c) shows silicon microposts etched via photolithography, (d) shows Krytox®-impregnated nanotexture, (e) shows Krytox®-impregnated superomniphobic, texture, and (f) shows Krytox®-impregnated microposts, respectively. It can be seen that the hollow part is filled with oils the surface height became constant and smooth.

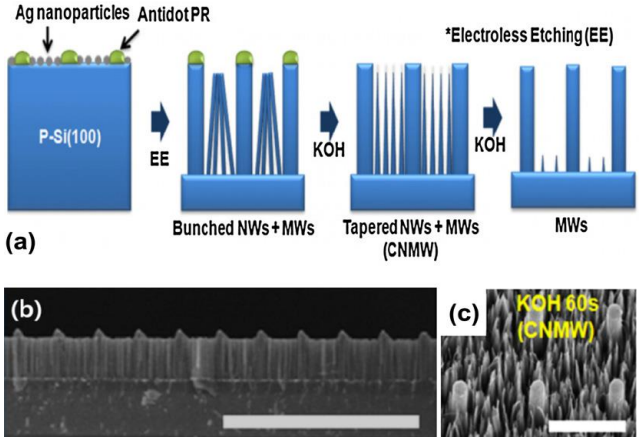

Fig. 13 Combination of metal-assisted chemical etching and another etching process. By choosing the particles or dots material deposited on the substrate, selective etching was carried out and subsequent anisotropic etching produce complex cross sectional profile as shown in (a). (b) shows the cross-sectional SEM photo, while (c) show the tilted view. Scale bar 10 μm [31].

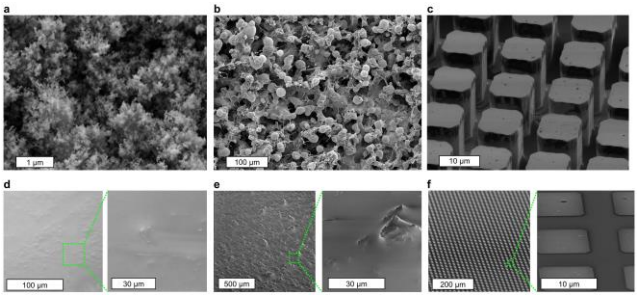

Fig. 14 Textured surfaces before and after lubricant impregnation. (a) alumina-silica nanotexture. (b) re-entrant superomniphobic texture. (c) microposts. (d) impregnated nanotexture. (e) impregnated superomniphobic, (f) impregnated microposts [32].

The mode of vapor condensation, dropwise or filmwise, is important in a discussion of heat transfer coefficient [32]. **Fig. 15** shows the estimated heat transfer coefficient *h* for various liquid that have different surface tension. In this study, three kinds of surfaces were compared: Bare silicon, fluorosilane, and nano-LIS surface, where "fluorosilane" denotes modified with low-surface energy material and "nano-LIS" denotes nanostructure impregnated with Krytox® oil, respectively. The points shows the experimental results. It is found that by modifying the surface, heat transfer coefficient increase drastically in case of fluorosilane. However, nano-LIS still has a possibility in improvement of the efficiency, because the pinning phenomenon is strongly affected by the texture without the oil.

It is easily predicted from the results shown in **Fig. 12** that parallel and smooth sidewalls can be used as an optic elements. Combining this etching process with precise lithography, the results can be applied X-ray zone plate elements. **Fig. 16** shows an example of such applications. Two by two array were produced with very fine regular structures. It is found that nanometer order structure were successfully produced [33].

3.1.4 Replication

Replication or casting is often used for texturing. Typical example is micro-channels used in microfluidics or micro-total analysis system (μ-TAS). In many cases, a reverted profile was produced in a photoresist with lithography, polydimethylsiloxane (PDMS) is poured onto it, and cured to obtain the required profile. Interesting is that PDMS structure is strongly adhered to glass or another PDMS structure after surface modification with plasma treatment. Without any sealant, any liquid can be fed into such channel or circuit, which enables stacked three-dimensional structure. Texturing of the PDMS has also been applied to control friction [34] or biocompatibility. It is quite interesting that polyvinylsiloxane (PVS) structure mimicking hexagonal structure found in nature were produced and have shown good frictional properties [35].

3.1.5 Laser

Historically, laser beam has been used for texturing [36]. The application fields has been tribology, mainly to decrease the coefficient of friction. Typical example is texturing of hydrodynamic thrust bearing [37][38].

Laser texturing have been often applied to texturing for hard disk drive. The head of the drive flies on a platter (disk) during its rotation keeping nm-order narrow gap. The principle is the hydrodynamic pressure between the head and platter. Thus, both of the head and platter should be precisely finished. However, mirror finished head may stick on platter while it stopped. This phenomena due to meniscus attraction is called stiction, and often observed in fabrication of micro-mechanism. To avoid this stiction, roughened area is intentionally produced in shipping zone on a platter (disk) while keeping the mirror finish on other area as shown in **Fig.17** [39].

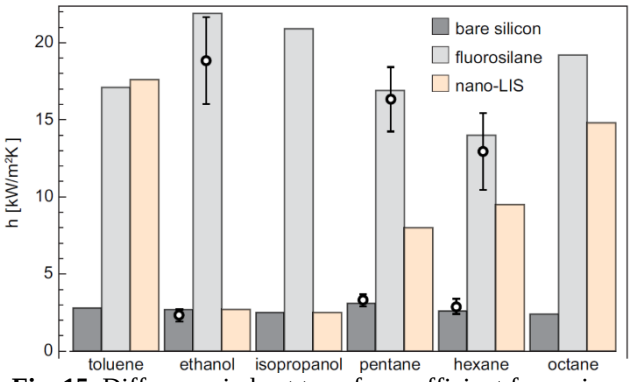

Fig. 15 Difference in heat transfer coefficient for various medium with different surface tension. [32].

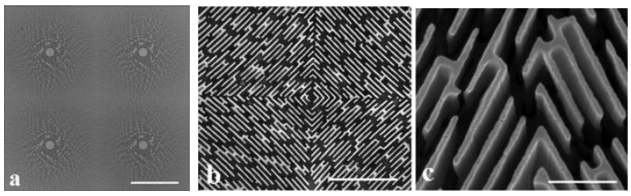

Fig. 16 Zone plate diffraction optics. 2 × 2 array of spiral zone plates patterned using electron beam lithography and lift-off. (b) The center portion of the array with silicon features etched. (c) A high magnification of the etched features. Scale bars are (a) 15 mm, (b) 2 mm, and (c) 500 nm. [33].

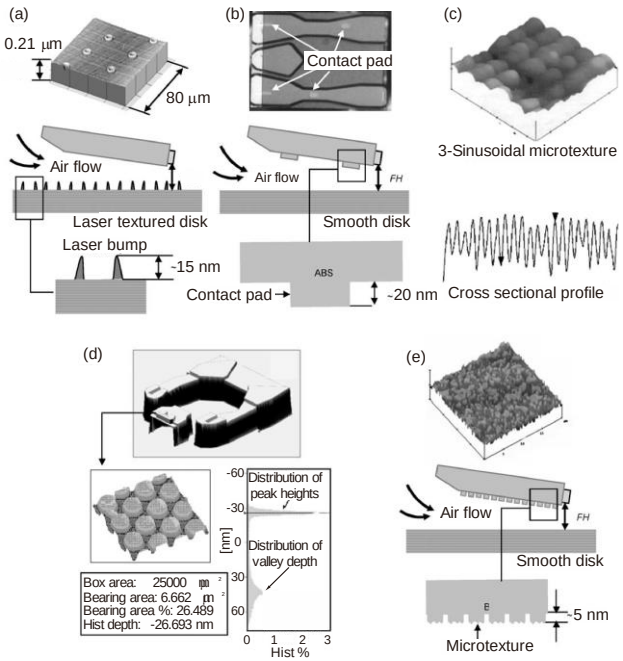

Fig. 17 Tribology at hard-disk interface. (a) laser textured disk, (b) slider with contact pad, (c) pseudo-sinusoidal textured pad, (d) subtractive slider texturing, (f) preferentially texture slider [39] (partially modified).

Femtosecond laser is one of the short pulse lasers and it is quite interesting that depth control can be possible [6], while traditional laser have been applied often for trimming of sheet material. It is furtherly interesting that regular patterns can be obtained after irradiating the laser.

Fig. 18 shows one of the results on titanium surface. Regular stripe or ripple structure can be obtained [40].

The mechanism has not been fully made clear and still discussed considering harmonic generation [41], and interference between laser light and surface plasmon polaritons [42]. This kind of regular structure is referred as laser-induced periodic surface structures (LIPSS).

Combining with scanning motion, laser texturing can produce various complex structures as shown in **Fig. 19** [40]. Minimum structural dimension is determined by the laser beam diameter, but, ideally, nanostructure can be fabricated on a structure, thus, micro-/nano-hierarchical structure is expected.

Fig. 20 shows a hierarchical structure on a silicon substrate. It looks like the structure on a lotus leaves (Fig.2), nanostructure is observed on micrometer structure. This kind of structure is often referred as "black silicon" and it is well known that the surface emits light, exactly "luminescence", as well as it absorbs light well [43]. Thus, electromagnetic function was attained with texturing.

3.2. Bottom up Processes

Contrarily to the top down processes, bottom up processes do not depend on the copying rule, but on self-organizing nature which proceed in parallel. The advantage is the high resolution up to molecular level. However they have drawback of randomness in the structure. To overcome this drawback, additional top down process have been recently applied.

3.2.1 Anodic Oxidation of Aluminum

Porous alumina can be obtained by anodic oxidation of aluminum [44]. Regularly allocated parallel pores can be obtained.

According to [45], the anodization process can be categorized into two regimes. **Fig. 21** shows the relationship between anodization voltage and distance between the pores. Depending on the applied voltage, the distance can be controlled. The difference between mild anodization (MA) and hard anodization (HA) is not only the pitch but the anodization speed or film growth rate. By changing the regime to HA, the growth rate can be ten times higher than the MA regime as shown in **Table 3**. In addition to the growth rate, other parameters become different. Special attention should be paid in the selection of these conditions.

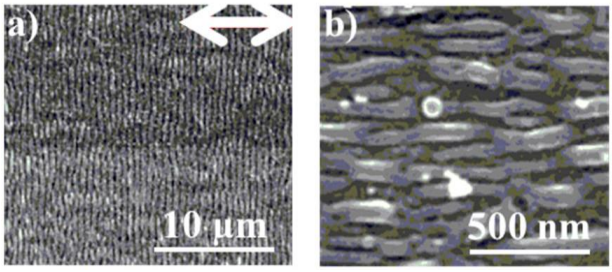

Fig. 18 SEM images of (a) low-spatial-frequency LIPSS (LSFL) and (b) high-spatial frequency LIPSS (HSFL) on Ti irradiated with 790 nm fs laser. The double-sided arrow indicates the polarization of the laser [40].

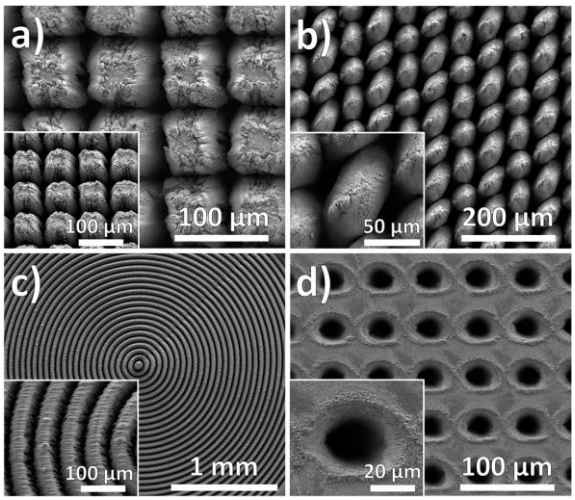

Fig. 19 Precisely patterned texture with laser. (a) square pillar, (b) parallelogram structures in a hexagonal arrangement, (c) circular grooves, and (d) micro hole pattern on Cu [40].

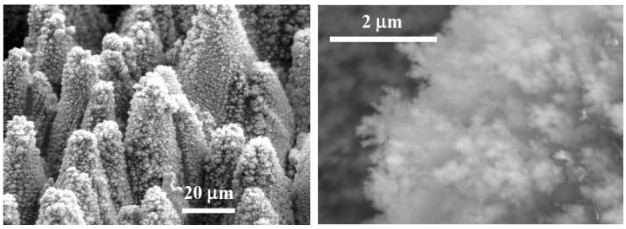

Fig. 20 SEM pictures of the black silicon surface with low magnification (a) and high magnification (b) [43].

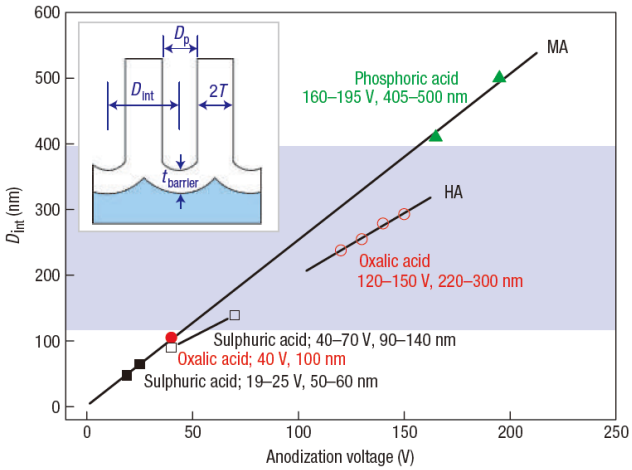

Fig. 21 Relationship between anodization voltage and pitch between pores. Pitch can be controlled with anodization voltage crossing hard anodization (HA) and mild anodization (MA) [45].

Table 3 Comparison of the properties between mild anodization and hard anodization in 0.3M $H_2C_2O_4$ (1 ◦C). Rewrited from [45]

Factors	MA	HA
Voltage (V)	40	110–150
Current density (mA cm^{-2})	5	30–250
Film growth rate (μmh^{-1})	2.0 (linear)	50–70 (nonlinear)
Porosity (%)	10	3.3–3.4
Interpore distance (nm)	100	220–300

Fig. 22 shows an experimental results which combines hard anodization and mild anodization. Fig. (a) shows the scheme, the initiation points of anodization were determined with imprinting dots on the substrate. Then, mild anodization or hard anodization were carried out periodically to change the diameter. Repeating these cycles, deep pores with modulated diameter were produced. It is also confirmed that pore diameter changed as intended while achieving high aspect ratio over 1,000. Regular hexagonal packed structure can be confirmed from top- and bottom-view observation results.

Regular nanopores has been applied to various field. An example is patterned media to improve the density of stored information of hard disk drive.

3.2.2 Self-Assembly of Particles

Fine particles can be assembled on a substrate without any complex control. Typical method is dip-coating in which a hydrophilic substrate is drawn up from a aqueous suspension in which fine particles are dispersed. The principle of self-assembly is the meniscus attraction between the particles after spreading and drying of suspension [46]. Tuning the conditions, hexagonally packed assembly in monolayer can be obtained. Some applications has been discussed [47].

Site selective self-assembly has been also tried with dip coating process as shown in **Fig.23**. In this case, preparation is required such as wettability patterning to limit the spreading of suspension that contains particles. Site selective assembly is also possible by using dispenser. In this case, pattern is applied by the lateral relative motion between the substrate and dispenser nozzle [48][49]. **Fig. 24** shows an example of linear assembly. Silica particles (ϕ1 μm) was assembled along lines of which width was about 17 μm. It is found that monolayer and packed structure was obtained. Ink-jet printing is another option to produce site-selective assemblies [50]. The assembled particles can be used as an etching mask [51] as well as a mask for lithography. The assembly can be used as abrasive tools [48][49].

3.2.3 Block Copolymer

Various complex structure can be produced by using block copolymer. The principle is attraction or repellant action in molecular level and regular structures are obtained without complex control. **Fig. 25** shows the variations of attainable three dimensional configuration, where character S denotes spheres or isolated dot. C denotes cylinder which have parallel tubes. G denotes gyroid which interconnect complex three dimensional locations. L denotes lamellae which denotes parallel planes. G', C', and S' denote complementally patterns of G, C, and S, respectively [52][53][54][55].

Fig. 26 shows a SEM observation result of cylinder type dots produced by block copolymer. It can be seen from the inset magnified view that dot pattern is not necessarily regular but have randomness. This regular area is often called "domain" and equivalent with a crystal grain in polycrystalline material. To eliminate this randomness, additional process shown in Fig. 22(a) is required to improve the accuracy of the pattern. This is the combination of bottom up process and top down processes.

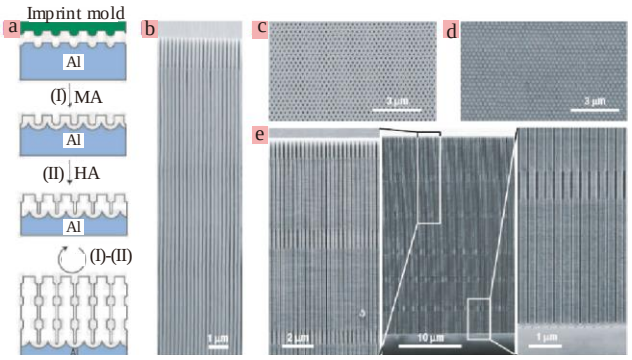

Fig. 22 Long-range ordered alumina membranes with modulated pore diameters. a: scheme of the process, b: SEM micrograph showing a cross-section of anodic alumina (pitch 210 nm). c,d: SEM micrographs showing the top and bottom view of the hexagonal arrangement of the nanopores. e: SEM micrographs showing the cross-section view of the corresponding sample with modulated pore diameters [31] (partially modified).

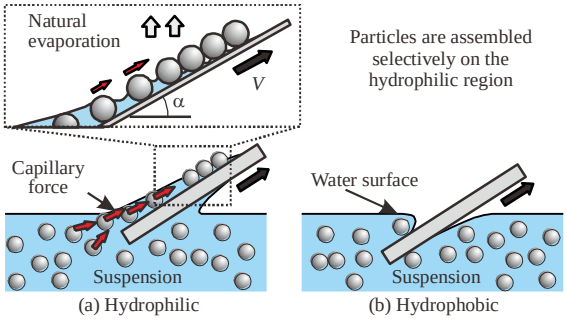

Fig.23 Dip coating of particles with aqueous suspension. Particles assembled only on hydrophilic area producing packed structure due to meniscus force between particles.

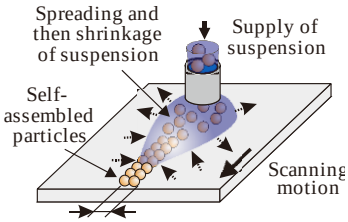

(a) Dip coating of particles with a dispenser. The suspension once spread and then shrink with the evaporation of solvent.

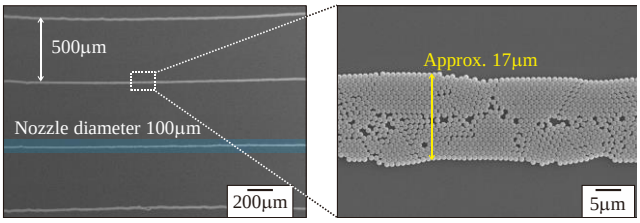

(b) Monolayer assembly along parallel pattern. ϕ1 μm silica particles.

Fig. 24 Self-assembled particles with a dispenser.

Fig. 27 shows a network structure made of block copolymer. Blending poly (styrene-b-isoprene) (PS/PI) diblock copolymer and polystyrene homopolymer. Complicated structure was once produced and then polyisoprene networks were removed selectively using ozonolysis. Fig (c) shows a solid model and in (d), the bright domain corresponds to the PS matrix, and the gray and dark phases correspond to the degraded PI phase [55].

Specific patterning with block copolymer has been applied to production of electric circuit [56].

3.3. Surface Modification Process

Depositing or modifying the surface with specific material, its functionality can be changed. The thickness can be minimized to molecular level (sub-nm order). Thus, this process can change the functionality without changing the original dimension or profile. Recently, organic material deposition is often applied.

3.3.1 Inorganic Materials

Inorganic materials have been mainly applied to improve tribological properties [57][58]. Carbon nanotubes (CNTs) or other carbon materials like carbon onions are often applied in addition to diamond like carbon (DLC). However, fixation of CNTs is one of the problems. In case of DLC, relaxation of high residual stress is another problem.

By choosing depositing material as silver particle, antibacterial surfaces can be obtained.

3.3.2 Organic Materials

Some kinds of polymers provide specific functions based on special material design. However, it is not easy to fix such materials on a rigid surface as metals. By using special bonding mechanism like Au-thiol and siloxane bonding, functional polymer can be fixed or grafted strongly. By modifying the molecular end-group on another side of these molecules, various functions can be attained while extending the life of the function. In some special cases, biocompatibility can be improved.

Fig. 28 shows the application example in which special polymer has been developed [60][61][62] and utilized to artificial joint [63]. In this case, special grafting process has been developed.

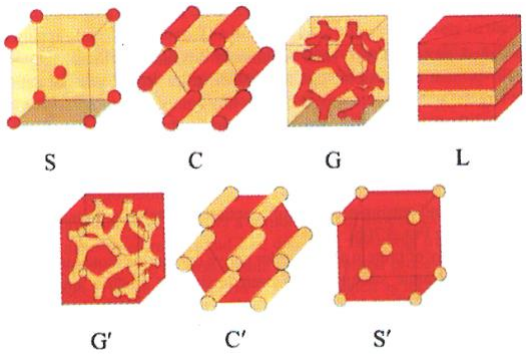

Fig. 25 Variation of three dimensional regular structures using block copolymer. [52].

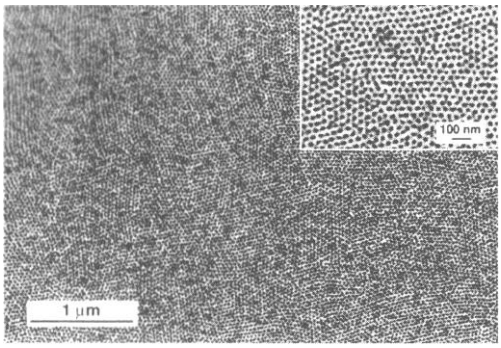

Fig. 26 Nano pillar assembly in copolymer[56].

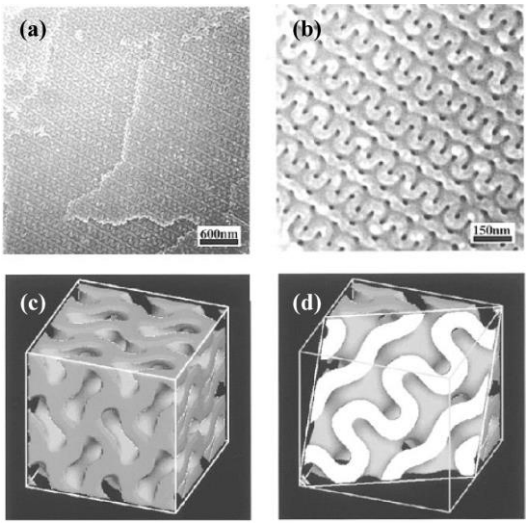

Fig. 27 SEM micrographs showing a bicontinuous nanochannel in the matrix of PS with two different magnifications ((a), (b)) and computer graphics of a double gyroid network: (c) a 3D view and (d) a 2D intersection cut along the (211) direction. [55].

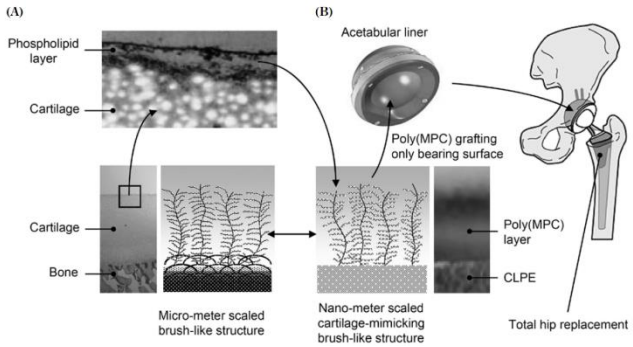

Fig. 28 Artificial joint utilizing grafted polymer. (A) shows interface between cartilage and polymer. (B) shows the schematics of artificial joint with grafted polymer [63].

4. Conclusion

Functional texture design and processes for its realization were surveyed. Bioinspired or biomimetic design is one of the important options. This idea can be applied to material structure design as well as surface functions.

Wide spectrum of processes were also introduced. Non-traditional physical or chemical processes are often applied for texturing.

Thus, variety of knowledge and experience are required both for products designers and process designers. Collaborative work will be important crossing over the boundary of traditional disciplines.

REFERENCES:

[1] K. Autumn, How Gecko Toes Stick, American Scientist, 94, 2006, pp. 124–132.

[2] P. Forbes, The Gecho's Foot, Harper-Collins Pub., 2007

[3] A. Nakajima, Control of Solid Surfaces, Uchida Rokakuho Publishing, 2007 (in Japanese).

[4] R. Bappert, S. Benner, B. Haecker, U. Kern, G. Zweckbronner, Bionik, Landesmuseum für Tecknik und Arbeit in Mannheim, 1998.

[5] M. Shimomura, New Trends in Next Generation Biomimetic Material Technology: Learning from Biodiversity, Science & Technology Trends Quarterly Review, NISTEP Science & Technology Foresight Center, 037, 2010, pp.53–75.

[6] C. J. Evans and J. B. Bryan, "Structured", "Textured" or "Engineered" Surfaces, Annals of CIRP, 48, 2, 1999, pp.541–556.

[7] S. Shibuichi, T. Onda, N. Satoh, K. Tsujii, Super Water-Repellent Surfaces Resulting from Fractal Structure, J. Phys. Chem., 100, 1996, pp. 19512–19517.

[8] T. Onda, S. Shibuichi, N. Satoh, K. Tsujii, Super-Water Repellent Fractal Surfaces, Langmuir, 12, 8, 1996, pp. 2125–2127.

[9] A. B. D. Cassie and S. Baxter, Wettability of Porous Surface, Trans. Faraday Soc., 40, 1944, pp. 546–551.

[10] J. Bico, U. Thiele, and D. Quere, Wetting of textured surfaces, Colloids and Surfaces, A: Physicochemical and Engineering Aspects 206, 2002, pp. 41–46.

[11] Y. Inoue, Y. Yoshimura, Y. Ikeda, A. Kohno, Effects of Roughness and Chemical Composition of an Ar Ion-Implanted Fluorine-Polymer on Water Repellency, Journal of The Surface Finishing Society of Japan Vol. 51, No. 5, 2000, pp. 512–517 (in Japanese).

[12] W. Chen, A. Y. Fadeev, M. C. Hsieh, D. Oener, J. Youngblood, and T.J. McCarthy, Ultrahydrophobic and Ultralyophobic Surfaces: Some Comments and Examples, Langmuir, 15, 10, 1999, pp. 3395–3399.

[13] M. Miwa, A. Nakajima, A. Fujishima, K. Hashimoto, and T. Watanabe, Effects of the Surface Roughness on Sliding Angles of Water Droplets on Superhydrophobic Surfaces, Langmuir, 16, 13, 2000, pp. 5754–5760.

[14] T-S. Wong, S. H. Kang, S. K. Y. Tang, E. J. Smythe, B. D. Hatton, A. Grinthal and J. Aizenberg, Bioinspired self-repairing slippery surfaces with pressure-stable omniphobicity, Nature, 22, 477, 2011, pp. 443–447.

[15] A. Tuteja, W. Choi, J. M. Mabry, G. H. McKinley & R. E. Cohen Robust omniphobic surfaces. Proceedings of the National Academy of Sciences, 105, 2008, pp. 18200–18205.

[16] E. Brinksmeier, R. Gläbe, Lars Schönemann Review on diamond-machining processes for the generation of functional surface structures, CIRP Journal of Manufacturing Science and Technology 5, 2012, pp.1–7.

[17] E. Brinksmeier, O. Riemer, R. Gläbe, B. Lünemann, C.v. Kopylow, C. Dankwart, A. Meier, Submicron functional surfaces generated by diamond machining, CIRP Annals - Manufacturing Technology 59, 1, 2010, pp. 535–538.

[18] S.R. Patterson, E.B. Magrab, Design and testing of a fast tool servo for diamond turning, Precision Engineering, Volume 7, Issue 3, July 1985, pp. 123–128.

[19] T. A. Dow, M. H. Miller, P. J. Falter, Application of a fast tool servo for diamond turning of nonrotationally symmetric surfaces, Precision Engineering, Volume 13, Issue 4, 1991, pp. 243–250.

[20] D. G. Thakur, B. Ramamoorthy, L. Vijayaraghavan, Effect of cutting parameters on the degree of work hardening and tool life during high-speed machining of Inconel 718, International Journal of Advanced Manufacturing Technology, 59, 5-8, 2012, pp 483–489

[21] Y-L. Chen, S. Wang, Y. Shimizu, S. Ito, W. Gao, B-F. Ju, An in-process measurement method for repair of defective microstructures by using a fast tool servo with a force sensor, Precision Engineering, Vol. 39, 2015, pp. 134–142.

[22] K. Salonitis, On surface grind hardening induced residual stresses, Procedia CIRP 13, 2014, pp. 264–269.

[23] D. Meyer, E. Brinksmeier, F. Hoffmann, Surface hardening by cryogenic deep rolling, Procedia Engineeting, 19, 2011, pp. 258–263.

[24] X. Wang, K. Adachi, K. Otsuka, K. Kato, Optimization of the surface texture for silicon carbide sliding in water, Applied Surface Science 253, 2006, pp. 1282–1286.

[25] H. Seidel, L. Csepregi, A. Heuberger, H. Baumgärtel , Anisotropic Etching of Crystalline Silicon in Alkaline Solutions I. Orientation Dependence and Behavior of Passivation Layers, Journal of Electrochemical Society, Vol. 137, No. 11, 1990, pp. 3612–3626.

[26] E. Vazsonyi, K. De Clercq, R. Einhaus, E. Van Kerschaver, K. Said, J. Poortmans, J. Szlufcik, J. Nijs, Improved anisotropic etching process for industrial texturing of silicon solar cells, Solar Energy Materials and Solar Cells, Volume 57, Issue 2, 26, 1999, pp. 179–188.

[27] Y. He, C. Jiang, H. Yin, J. Chen, W. Yuan, Superhydrophobic silicon surfaces with micro–nano hierarchical structures via deep reactive ion etching and galvanic etching, Journal of Colloid and Interface Science 364, 2011, pp.219–229.

[28] Z. Huang, N. Geyer, P. Werner, J. de Boor , and U. Gösele, Metal-Assisted Chemical Etching of Silicon: A Review, Advanced Materials. 23, 2011, pp. 285–308.

[29] N. Geyer, B. Fuhrmann, Z. Huang, J. de Boor, H. S. Leipner, and P. Werner, Model for the Mass Transport during Metal-Assisted Chemical Etching with Contiguous Metal Films As Catalysts, Journal of Physical Chemistry C, 116, 2012, pp. 13446–13451.

[30] X. Li, Metal assisted chemical etching for high aspect ratio nanostructures: A review of characteristics and applications in photovoltaics, Current Opinion in Solid State and Materials Science 16, 2012, pp. 71–81.

[31] X. Geng, Z. Qi, M. Li, B. K.Duan, L. Zhao, P. W. Bohn, Fabrication of antireflective layers on silicon using metal-assisted chemical etching with in situ deposition of silver nanoparticle catalysts, Solar Energy Materials & Solar Cells, 103,2012, pp. 98–107.

[32] K. Rykaczewski, A. T. Paxson, M. Staymates, M. L. Walker, X. Sun, S. Anand, S. Srinivasan, G. H. McKinley, J. Chinn, John H. J. Scott & K. K. Varanasi, Dropwise Condensation of Low Surface Tension Fluids on Omniphobic Surfaces, Scientific Reports, 4, 4158, 2014.

[33] R. C. Tiberio, M. J. Rooks, C. Chang, C. F. Knollenberg, E. A. Dobisz, A. Sakdinawat, Vertical directionality-controlled metal-assisted chemical etching for ultrahigh aspect ratio nanoscale structures, Vacuum Science and Technolgies B, Nanotechnol Microelectron Mater Process Meas Phenom, 32, 6, 2014, pp. 06FI01-1–06FI01-5.

[34] B. He, W. Chen, Q. J. Wang, Surface Texture Effect on Friction of a Microtextured Poly(dimethylsiloxane) (PDMS), Tribology Letter, 31, 2008, pp.187–197.

[35] A. Tsipenyuk and M. Varenberg, Use of biomimetic hexagonal surface texture in friction against lubricated skin, Journal of the Royal Society Interface.2014, 0113.

[36] I. Etsion, State of the Art in Laser Surface Texturing, Journal of Tribology, Trans ASME, 127, 2005, pp.248–253.

[37] A. Dunn, J. V. Carstensen, K. Wlodarczyk, E. B. Hansen, J. Gabzdyl, P. M. Harrison, J. D. Shephard, D. P . Hand, Nanosecond laser texturing for high friction applications, Optics and Lasers in Engineering, 62, 2014, pp.9–16.

[38] U. Pettersson, S. Jacobson, Influence of surface texture on boundary lubricated sliding contacts, Tribology International 36, 2003, pp. 857–864.

[39] A.Y. Suh, S.-C. Lee and A.A. Polycarpou, Adhesion and friction evaluation of textured slider surfaces in ultra-low flying head-disk interfaces, Tribology Letters, Vol. 17, No. 4, 2004, pp. 739–749.

[40] K. M. T. Ahmmed, C. Grambow and A-M. Kietzig, Fabrication of Micro/Nano Structures on Metals by Femtosecond Laser Micromachining, Micromachines, 5, 2014, pp. 1219–1253; doi:10.3390/mi5041219.

[41] Borowiec, A.; Haugen, H.K. Subwavelength ripple formation on the surfaces of compound semiconductors irradiated with femtosecond laser pulses. Appl. Phys. Lett. 2003, 82, pp. 4462–4464.

[42] Huang, M.; Zhao, F.; Cheng, Y.; Xu, N.; Xu, Z. Origin of laser-induced near-subwavelength ripples: Interference between surface plasmons and incident laser. ACS Nano 2009, 3, pp. 4062–4070.

[43] A. Serpengüzel, A. Kurt, I. Inanç, J. E. Cary, and E. Mazur, Luminescence of black silicon, Journal of Nanophotonics, Vol. 2, 021770 (21 February 2008)

[44] K. Nishio, T. Yanagishita, S. Hatakeyama, M. Maekawa, and H. Masuda, Fabrication of Ideally Ordered Anodic Porous Alumina with Large Area by Vacuum Deposition of Al onto Mold, Journal of vacuum science & technology. B, 26, L10, 2008.

[45] W. Lee, R. Ji, U. Gösele and K. Nielsch, Fast fabrication of long-range ordered porous alumina membranes by hard anodization, Nature materials, 5, 2006, pp.741–747.

[46] N. D. Denkov, O. D. Velev, P.A. Kralchevsky, I. B. Ivanov, H. Yoshimura and K. Nagayama, Two dimensional crystallization, Nature, 361, 1993, p. 26.

[47] A. S. Dimitrov and K. Nagayama, Continuous convective assembling of fine particles into morphocolored two-dimensional arrays, Langmuir 12, 1996, pp.1303–1311.

[48] N. Moronuki, W-R Zhang, Patterned Self-Assembly of Fine Particles and Its Application to Polishing Tool, Journal of Advanced Mechanical Design, Systems, and Manufacturing, 6, 6, 2012, pp. 792–799.

[49] N. Moronuki, A. Kaneko, and K. Takada, Patterned Self-Assembly of Fine Particles as a Proposal of Precisely Allocated Cutting-Edge Tool, International Journal of Automation Technology, 5, 3, 2011, pp.289–293

[50] J. Park, et al., Control of Colloidal Particle Deposit Patterns within Picoliter Droplets Ejected by Ink-Jet Printing, Langmuir, 22, 2006, pp.3506–3513.

[51] H. Kobayashi, N. Moronuki, and A. Kaneko, Self-assembly of Fine Particles Applied to the Production of Antireflective Surfaces, International Journal of Precision Engineering and Manufacturing, Vol. 9, No.1, 2008, pp.25–29.

[52] H-E. Schaefer, Nanoscience, Springer, 2010.

[53] H.-A. Klok, S. Lecommandoux, Supramolecular Materials via Block Copolymer Self-Assembly, Advanced Materials, 13, 16, 2001, pp.1217–1229

[54] S. C. Warren, L. C. Messina, L. S..Slaughter, M. Kamperman, Q. Zhou, S. M. Gruner, F. J. DiSalvo, U. Wiesner , Ordered Mesoporous Materials from Metal Nanoparticle–Block Copolymer Self-Assembly, Science 27, Vol. 320 No. 5884, 2008, pp. 1748–1752.

[55] C. Park, J. Yoon, E. L. Thomas, Enabling nanotechnology with self assembled block copolymer patterns, Polymer, 44, 2003, pp. 6725–6760.

[56] K. W. Guarini, C. T. Black, K. R. Milkove and R. L. Sandstrom, Nanoscale patterning using self-assembled polymers for semiconductor applications, J. Vac. Sci. Technol. B 19, 2001, pp. 2784–2787.

[57] X. Deng, H. Kousaka, T. Tokoroyama, N. Umehara, Deposition and tribological behaviors of ternary BCN coatings at elevated temperatures, Surface and Coatings Technology 259, 2014, pp. 2–6.

[58] X. Deng, H. Kousaka, T. Tokoroyama, N. Umehara, Tribological behaviors of tetrahedral amorphous carbon (ta-C) coatings at elevated temperature, Triblogy International, 75, 2014, pp. 98–103.

[59] T. Hashimoto, K. Tsutsumi, and Y. Funaki , Nanoprocessing Based on Bicontinuous Microdomains of Block Copolymers: Nanochannels Coated with Metals, Langmuir, 13, 26, 1997, pp. 6869–6872.

[60] T. Moro, Y. Takatori, K. Ishihara, T. Konno, Y. Takigawa, T. Matsushita, U. Chung, K. Nakamura and H. Kawaguchi, Surface grafting of artificial joints with a biocompatible polymer for preventing periprosthetic osteolysis, Nature Materials 3, 2004, pp. 829–836.

[61] T. Moro, Y. Takatori, K. Ishihara, K. Nakamura, H. Kawaguchi. Grafting of biocompatible polymer for longevity of artificial hip joints, Clinical orthopaedics and related research, 453, 2006, pp. 58–63.

[62] T. Moro, H. Kawaguchi, K. Ishihara, M. Kyomotoa, T. Karita, H. Ito, K. Nakamura, Y. Takatori, Wear resistance of artificial hip joints with poly(2-methacryloyloxyethyl phosphorylcholine) grafted polyethylene: Comparisons with the effect of polyethylene cross-linking and ceramic femoral heads, Biomaterials, Volume 30, Issue 16, 2009, pp. 2995–3001.

[63] Y. Ishikawa, K. Hiratsuka, T. Sasada, Role of water in the lubrication of hydrogel, Wear, Volume 261, Issues 5–6, 2006, pp. 500–504.

Name:
Nobuyuki Moronuki

Affiliation:
Professor, Tokyo Metropolitan University

Address:
6-6 Asahigaoka, Hino-shi, Tokyo 191-0065, Japan

Brief Biographical History:
1989 Received Doctor degree from Tokyo Metropolitan University
1990- Associate Professor of Tokyo Metropolitan University
2005- Professor of Tokyo Metropolitan University

Main Works:
- Micro-/Nano-structuring based on self-assembly of particles to improve surface functionality in biomedical applications, Procedia Engineering, 19, 2011, pp. 276–281.
- Self-assembly of Fine Particles Applied to the Production of Antireflective Surfaces, International Journal of Precision Engineering and Manufacturing, Vol. 9, No.1, 2008, pp.25-29.

Membership in Academic Societies:
- The Japan Society of Mechanical Engineers (JSME)
- The Japan Society for Precision Engineering (JSPE)
- The european society for precision engineering and nanotechnology (euspen)